Effect of pressure on the atomic volume of Ga and Tl up to 68 GPa

Olaf Schulte and Wilfried B. Holzapfel
FB 6 Physik, Universität-GH-Paderborn, 33095 Paderborn, Germany
(Received 26 December 1995; revised manuscript received 15 October 1996)

The elemental metals Ga and Tl are studied under pressure in a diamond anvil cell by energy dispersive x-ray diffraction. While Tl remains in the high-pressure $cF4$ structure up to the highest pressures achieved, several phase transitions are observed in Ga. Different equation-of-state (EOS) forms are fitted to the experimental data. A detailed analysis of the data shows that a simple first-order EOS form can describe the isothermal pressure-volume behavior of all the phases for Ga as well as for Tl. Furthermore, a comparison of the structural behavior under pressure is made for all the group-IIIA elements of the Periodic Table. [S0163-1829(97)05413-1]

I. INTRODUCTION

Progress in pressure generation with diamond anvil cell (DAC) and suitable x-ray diffraction techniques resulted in the unique opportunity to study not only equations of state (EOS) but also all the structural parameters of crystalline solids in a pressure range previously accessible only to shock wave experiments.[1] Systematic investigations of the high-pressure behavior of the metallic elements have been concentrated previously on alkali[2–4] and earth alkali metals,[5–9] on the transition elements,[10,11] and on the lanthanides.[12–18] The group-IIIA elements, however, have been studied previously only in lower-pressure ranges, because no effects due to electronic transitions were expected in these cases.[19,20] More recent theoretical calculations of the phase stabilities for these elements[21–24] called also for experimental studies in an extended pressure range. For instance, studies on In up to 100 GPa gave evidence for an unexpected phase transition to an orthorhombic structure[25,26] and the theoretical prediction of a phase transition in Al from the low-pressure $cF4$ structure[27] to a $hP2$ structure around 100 GPa (Ref. 28) was not confirmed by recent x-ray investigations to 220 GPa.[29]

Furthermore, a comparison of the extended EOS data with different EOS forms allows for a discrimination between more or less suitable forms if accurate low-pressure data are also available for comparison with new data for the extended p-V regions. Thereby, the use of some specific forms[30] allows us to distinguish between simple and more complex compressional behavior[31–33] by comparison with ultimate asymptotic laws.[34] It has also been shown that one of these new forms is very useful to describe the pressure-volume behavior of high-pressure phases for which the volume at zero pressure, V_0, is usually unknown. This analysis illustrates finally with the use of all the present data of Ga and Tl together with literature data also for B, Al, and In some systematic trends of the group-IIIA elements and gives some hints for special contributions from filled and unfilled outer d-electron shells to the EOS behavior of these elements.

II. EXPERIMENTAL TECHNIQUE

Diffraction patterns of Ga and Tl were obtained by energy dispersive x-ray diffraction (EDXD) using either a conventional x-ray tube with a W anode and the conical slit system in the laboratory[35] or with synchrotron radiation at HASYLAB, DESY.[36,37] High pressure was generated by a diamond anvil cell[38,39] (DAC) with an Inconel X750 gasket. Beveled diamond anvils with an outer culet diameter of 400 μm and an inner flat diameter of 300 μm were used in the studies extending the pressure range beyond 50 GPa. Pressures were measured with the ruby luminescence technique[40] on the basis of the nonlinear pressure scale.[41] Liquid nitrogen or mineral oil were used as the pressure-transmitting medium with no significant differences. For low-temperature measurements the DAC was installed in a liquid nitrogen bath cryostat.[36]

III. EDXD RESULTS

A. Gallium

Investigations on Ga were performed up to 67 GPa at room temperature and up to 40 GPa at 150 K. In this pressure range, several phase transitions have been observed. Starting from the orthorhombic $oS8$ structure of α-Ga stable at ambient conditions,[42] four other modifications[19,20,43,44] have been observed in the earlier studies in the pressure range below 8 GPa. Typical diffraction patterns for the mixed phase region of β-Ga ($mS4$) and $cI12$-GaII and for the pure $tI2$-GaIII are shown in Fig. 1. In fact, the first spectrum in Fig. 1 for 19.8 GPa is typical for a pure $tI2$ sample obtained after decreasing the pressure from significantly higher pressures to reduce effects from phase mixing and ''texture,'' which refers here to nonideal intensity distributions among the allowed diffraction lines due to the occurrence of coarse crystalline grains and possible preferred orientations after recrystallizations in the different phase transitions. The next pattern in Fig. 1 taken after a further decrease of the pressure down to 15.2 GPa no longer contains any traces of the $tI2$-GaIII phase but cannot be indexed either to pure $cI12$-GaII. Most likely, it contains already minor admixtures of β-Ga ($mS4$) and, vice versa, the patterns at lower pessures are typical for a low-symmetry structure corresponding to mainly β-Ga ($mS4$) with possible admixtures still of $cI12$-GaII. Due to the well-known metastabilities in this low-pressure part of the Ga phase diagram,[19,24,44]

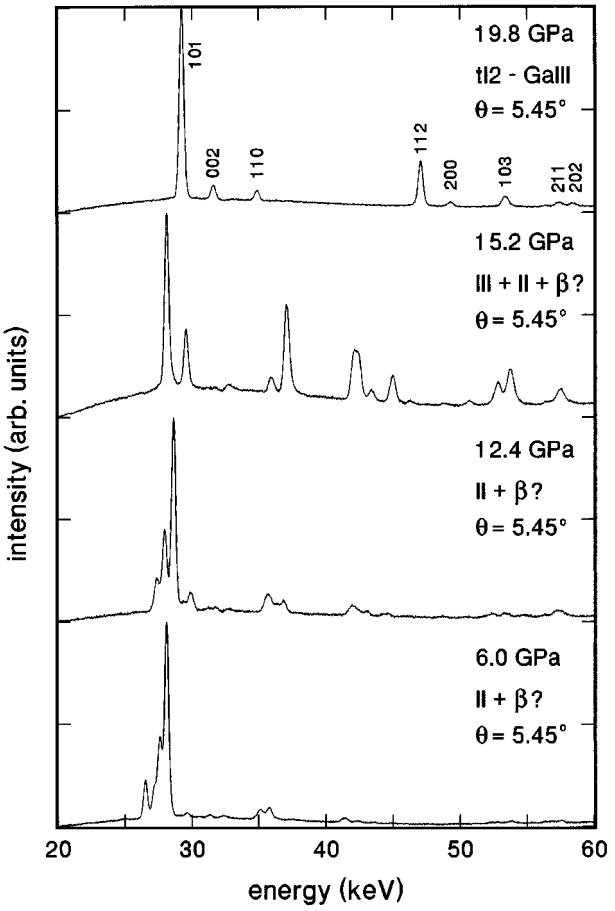

FIG. 1. Typical EDXD patterns for Ga in the low-pressure structures discussed in the text obtained with synchrotron radiation typically in 40 min with decreasing pressure.

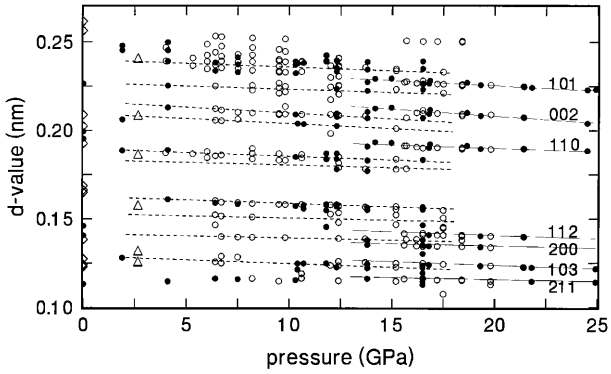

FIG. 2. Observed d values for Ga under pressure at ambient temperature. Solid circles refer to increasing pressure, open circles to decreasing pressure. The triangles represent the previous single-crystal data (Ref. 44) for GaII and the diamonds the ambient pressure data (Ref. 43) for β-Ga. The dashed and solid lines represent only guides to the eye and hkl values are given only for $tI2$-GaIII.

no equlibrium phase transition line could be determined for the low-pressure phases α, β, and GaII, and typically the effects of ''texture'' were even much stronger in the first pressure cycles of increasing pressure. For this reason, Fig. 2 illustrates first of all the different d spacings obtained on increasing and decreasing pressure with different symbols. Only lines with more than 5% intensity with respect to the strongest line in each pattern are represented in this plot. The intensities and positions were obtained thereby from least-squares fits of Gaussian profiles to the diffraction lines with the use of a specially adapted software.[45] Due to the large number of diffraction lines in the patterns of the mixed β-Ga+GaII region illustrated also in Fig. 2, it is clear that these patterns cannot be assigned to a pure $cI12$-GaII phase alone. For this reason, d values for the metastable β-Ga at ambient pressure as well as for $cI12$-GaII according to the literature data[42–44] are also shown in Fig. 2, whereby the pressure for the GaII data, which was not determined in the original measurement,[43] has been selected in such a way that the most dominant lines of GaII fit to the observed pattern. Obviously, many of the observed lines in the mixed β-Ga +GaII region can be assigned to one of these structures; however, due to the many lines and due to the (irreproducible) texture in the observed spectra, the indexing is not straightforward for the present data and further studies are in progress to elucidate the present theoretical picture,[24] which predicts that β-Ga ($mS4$) is only a metastable phase between α-Ga ($oF8$) and $cI12$-GaII at least at low temperatures.

Around 15 GPa on increasing pressure at ambient temperature, Ga transforms to the body-centered tetragonal $tI2$-GaIII phase. This $tI2$ structure is the same as for In at ambient pressure with a c/a ratio $>\sqrt{2}$ equivalent to a face-centered tetragonal structure with four atoms in the unit cell ($tF4$) and with an axial ratio just slightly larger than 1. This phase transformation together with its hysteresis is clearly documented in the plot of the d values from the whole series of diffraction patterns in Fig. 2.

The variations of the lattice parameters a and c and also of the atomic volume for $tI2$-GaIII under pressure are illustrated in Fig. 3. Obviously, the two axes show different compressibilities and c/a decreases. Figure 4 presents the variation of the c/a ratio for the $tI2$ structure with respect to the atomic volume V. At $V/V_0=0.61$ the value of c/a becomes $\sqrt{2}$, or, in the $tF4$ representation, $c/a=1$. From the few data points above 60 GPa it is not clear whether this change in c/a corresponds to a continuous or discontinuous approach to the special value of $\sqrt{2}$ in Fig. 4 or even to a possible crossover to $c/a<\sqrt{2}$ at higher pressures. However, structural systematics[19] with respect to the other heavier group-III metals In and Tl as well as theoretical predictions[24,46] give strong hints that the occurrence of the special $c/a=\sqrt{2}$ marks the stability of a new phase GaIV with $cF4$ structure as noted in Fig. 5.

These ambient temperature data together with measurements at lower temperatures were finally used to construct the extended pressure temperature phase diagram of Ga in Fig. 5. Thereby, the slope of the boundary between $tI2$-GaIII and $cF4$-GaIV has been estimated from an extrapolation of the c/a data taken at low temperature, showing an approach to the cubic value at 82 GPa and 150 K. The shaded area around this boundary represents the uncertainty of this extrapolation. The shaded area for the boundary between the phases $cI12$-GaII and $tI2$-GaIII, however, repre-

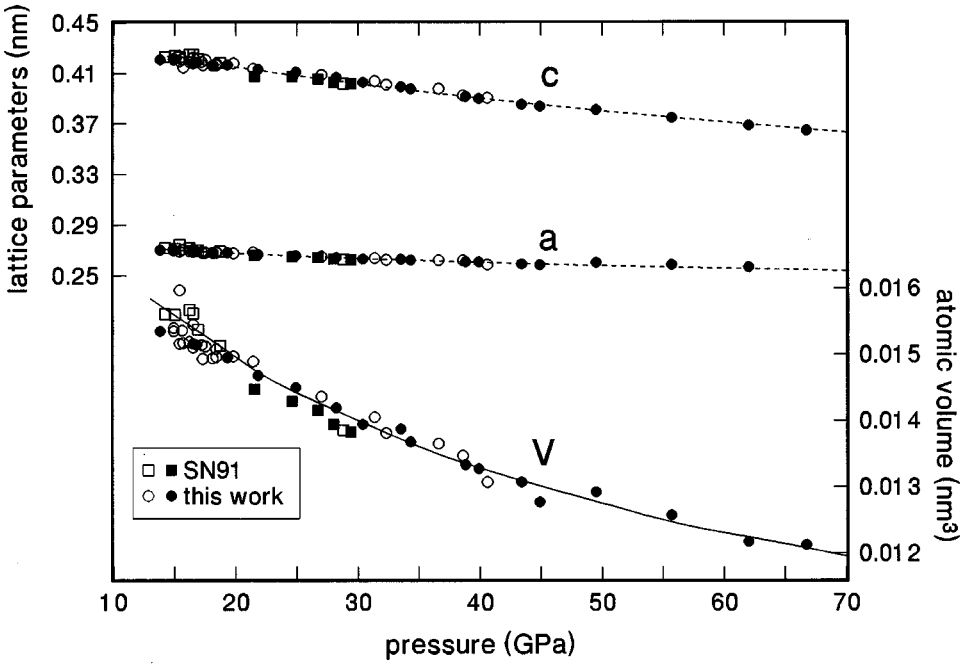

FIG. 3. Effect of pressure on the lattice parameters a and c and on the atomic volume for $tI2$-GaIII at ambient temperature. Solid circles refer to increasing pressure, open circles to decreasing pressure, and squares to the previous low-pressure EDXD measurements (Ref. 20). The dashed lines represent polynomial fits to the data of the lattice parameters. The solid line through the volume data resulted from these fits.

sents a region of hysteresis, whereby the solid and open symbols indicate the forward and backward transition points, respectively. The best estimate for the equilibrium phase boundary is illustrated by the strong dashed line.

B. Thallium

The structural behavior of Tl was studied up to 68 GPa with the observation of only $cF4$-TlII at pressures above 4 GPa. The results for the atomic volume under pressure are shown in Fig. 6 together with earlier data. To convert these earlier relative V/V_0 measurements to absolute atomic volume data, $V_0 = 0.028\,59$ nm^3 was used for the atomic volume at ambient conditions.[42] Obviously, reasonable agreement within the experimental accuracy is found for all the data from volumetric,[47,48] shock wave,[49] and angular dispersive x-ray diffraction[50] studies, as well as with our previous EDXD results[20] using a conventional x-ray source for the lower-pressure region.

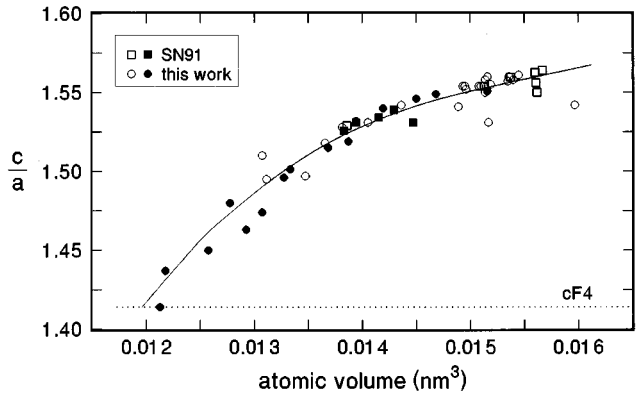

FIG. 4. Variation of c/a with respect to the atomic volume V for $tI2$-GaIII at ambient temperature with the same symbols for the data as in Fig. 3. The solid line represents the result of the polynomial fits for the lattice parameters, and the dotted line gives the c/a ratio for a $cF4$ structure.

IV. EOS FORMS FOR GROUP-IIIA ELEMENTS

In the past various procedures have been used to derive more or less physically justified analytic forms for the representation of p-V isotherms. These procedures have been discussed in a recent review[51] and also[33] with respect to the evaluation of EOS data for Zn, Cd, and Hg. Thereby, the most common second-order (two-parameter) forms originally given by Murnaghan,[52] Birch,[53] and Vinet *et al.*[54] were labeled MU2, BE2, and MV2, respectively, and some more recent forms[30,51] with the correct asymptotic limit at ultimate compression were labeled $H11$ and $H12$ to distinguish the corresponding first- and second-order forms.

Furthermore, a convenient ''linearization-scheme'' of the form $\eta(x) = \ln(p/p_{FG}) - \ln(1-x)$ was introduced[30] with $x = (V/V_0)^{1/3}$ and the (nonrelativistic) Fermi gas pressure $p_{FG} = a_{FG}(Z/V)^{5/3}$, which involves besides the atomic number Z and the atomic volume V only the characteristic constant $a_{FG} = \hbar^2/m_e(3/\pi)^{2/3}/20 = 23.37$ MPa nm^5.

With the literature data[29,49,55–61] for Al the corresponding $\eta(x)$ plot, Fig. 7, illustrates, first of all, that ''simple solids''[30] are characterized just by a linear η-x relation all

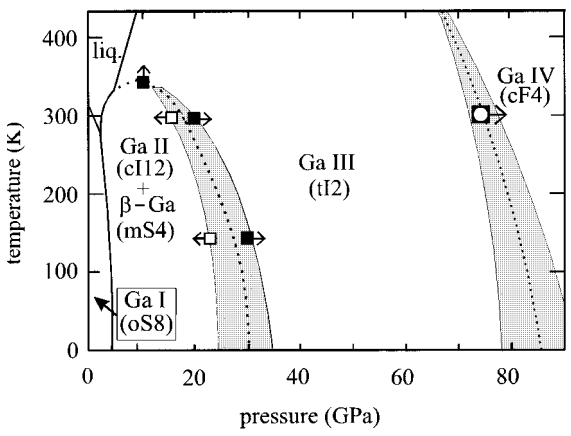

FIG. 5. Phase diagram for Ga. For details see text.

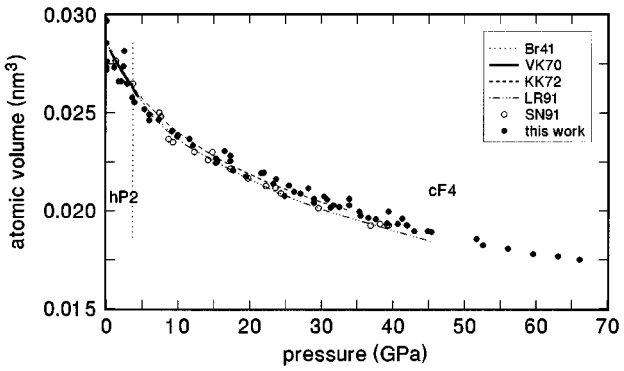

FIG. 6. EOS data of Tl at ambient temperature from the present study (solid circles) together with previous data from the literature [Br41 (Ref. 47), VK70 (Ref. 48), KK72 (Ref. 49), LR91 (Ref. 50), SN91 (Ref. 20)].

the way down to ambient conditions ($x=1$) from ultimate compression, $x \ll 0.01$, where relativistic effects have to be taken into account. Recent EDXD measurements[29] together with previous shock wave,[49,55,56] theoretical,[57–60] and ultrasonic[61] data illustrate that this group-IIIA element appears to be the most well-studied case which closely follows this linear relation. This linear relation corresponds directly to the first-order form $H11$ with only K_0 as free parameter. K_0', on the other hand, is thereby correlated to K_0 and V_0 through p_{FG_0} by the form $K_0' = 3 - \ln(3K_0/p_{\mathrm{FG}_0})$ as discussed in detail previously.[30,51] In fact, V_0 is thereby usually treated as a given value and not as a free parameter which then restricts the fitting just to the one parameter K_0.

This simple case can demonstrate most readily that extrapolations of most of the other empirical forms like MU2, BE2, or MV2 lead rather rapidly to strong divergences at strong compression with respect to the experimental and theoretical data, especially if the same (experimental) values are

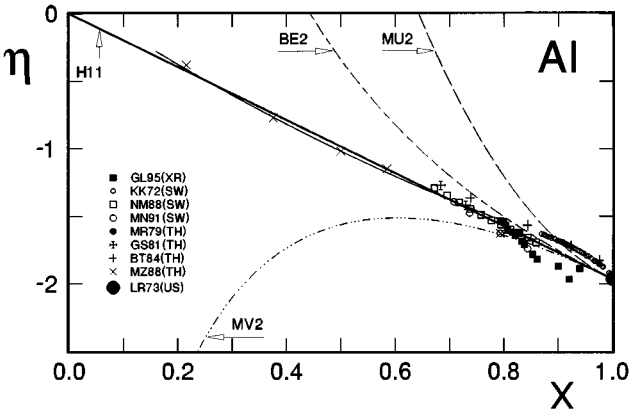

FIG. 7. EOS data for Al at ambient temperature from the literature [GL95 (Ref. 29), KK72 (Ref. 49), NM88 (Ref. 55), MN91 (Ref. 56), MR79 (Ref. 57), GS81 (Ref. 58), BT84 (Ref. 59), MZ88 (Ref. 60), LR73 (Ref. 61)] including shock wave (SW), x-ray diffraction (XR), and ultrasonic (US) measurements as well as theoretical (TH) data in an η-x representation using $\eta = \ln(p/p_{\mathrm{FG}}) - \ln(1-x)$. The linear interpolation $H11$ and different extrapolations MU2, BE2, and MV2 correspond to common EOS forms discussed in the text.

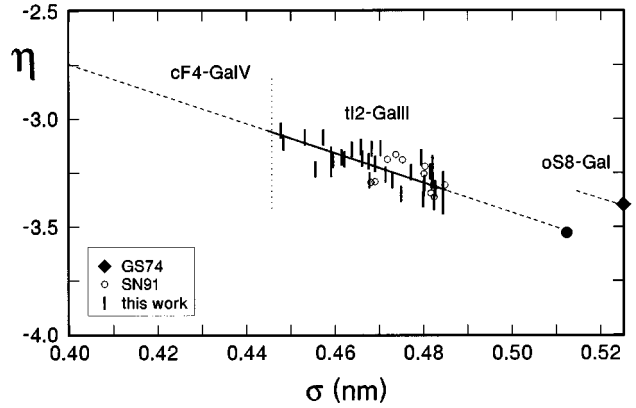

FIG. 8. EOS data for $tI2$-GaIII at ambient temperature with previous results [SN91 (Ref. 20)] together with data for α-Ga ($oS8$) [GS74 (Ref. 62)] in an η-σ representation using $\eta = \ln(p/p_{\mathrm{FG}}) - \ln(1-\sigma/\sigma_0)$ with the Fermi gas pressure p_{FG} and the parameter σ explained in the text.

used in all these forms for the ''free parameters'' K_0 and K_0'.

This observation stimulates the attempt to use the form $H11$ not only for low-pressure but also for high-pressure phases equally well for all the other group-IIIA elements just with the two parameters V_0 and K_0 adjusted by least-squares fitting. Thereby, one has to keep in mind that these two parameters are not directly measurable quantities for high-pressure phases, but nevertheless bear some direct physical meaning characterizing the metastable state of the high-pressure phase at ambient conditions.

For the comparison of different (high-pressure) phases of one given substance with different values of V_0 for each phase as well as for the comparison of EOS data for different substances with different values of Z and V_0, it is more convenient[30,51] to plot η versus σ using $\sigma = \sigma_0 x$ with $\sigma_0 = (3ZV_0/4\pi)^{1/3}$. In this case, one obtains (approximately) the same Thomas-Fermi slope for all the phases and sub-

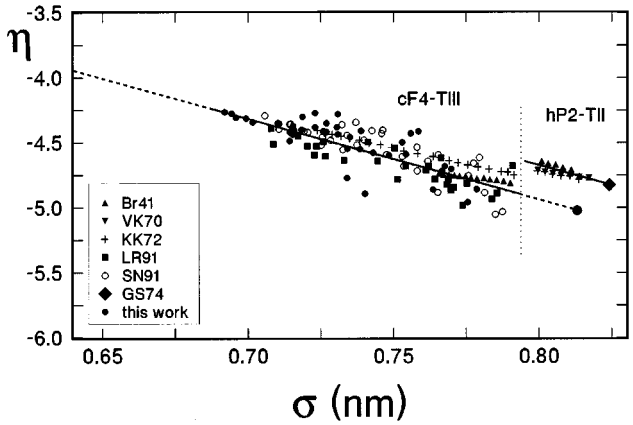

FIG. 9. EOS data for Tl at ambient temperature in an η-σ representation using $\eta = \ln(p/p_{\mathrm{FG}}) - \ln(1-\sigma/\sigma_0)$ with the Fermi gas pressure p_{FG} and the parameter σ explained in the text together with various data from the literature [Br41 (Ref. 47), VK70 (Ref. 48), KK72 (Ref. 49), LR91 (Ref. 50), SN91 (Ref. 20), GS74 (Refs. 62 and 63)].

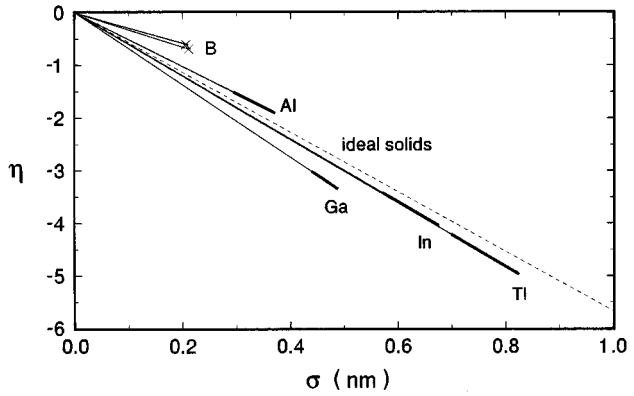

FIG. 10. EOS data for group-IIIA elements in an η-σ representation. The solid curves represent the range of the experimental data, thin lines represent interpolations, and the dotted line illustrates the average behavior of ''ideal'' solids (Ref. 30).

stances at ultimate compression. This will be shown later in Fig. 10 in the comparison of all the EOS data for the group-IIIA elements.

A. EOS data for Ga

The present EOS data for the high-pressure phase $tI2$-GaIII are represented in Fig. 8 in the form of an η-σ plot together with the one data point for $oS8$-GaI at ambient conditions corresponding to the given values[42,62] for V_0 and K_0 of this phase. The straight line interpolations of the form $H11$ for both of these phases represent the present best fits of this form to the data within the given accuracy. One may just note that the value $V_0(tI2\text{-GaIII})=0.0187(1)$ nm^3 is about 5% smaller than the value for $oS8$-GaI. The value for the bulk modulus, $K_0(tI2\text{-GaIII})=47(2)$ GPa, is significantly smaller than the corresponding (isothermal) value $K_0(oS8\text{-GaI})=56$ GPa from ultrasonic measurements[62] for the low-pressure phase $oS8$-GaI. The present value $K_0'(tI2\text{-GaIII})=5.4(1)$ can be compared only to $K_0'(oS8\text{-GaI})=5.1$ derived from the corresponding values for V_0 and K_0 by the use of the linear interpolation $H11$. Thereby, the numbers in brackets represent only the standard deviations of the least-squares fits for the form $H11$ with strongly correlated values for V_0, K_0, and K_0'. The standard deviation σ_V for the volume of the p-V data with respect to the fitted curve is thereby 1.9%, including the uncertainties in the pressure determination. Due to the strong correlation of the extrapolated values for V_0, K_0, and K_0' also in any fitting procedure of any other EOS form, not too much emphasis should be given to these actual values. In fact, the fit of a second-order Birch equation results even in a larger value for V_0, a smaller value for K_0, and an unreasonably large value for $K_0'>8$. Whether such unreasonable values are related to the instability of the high-pressure phase under these conditions or just to the wide extrapolation needed with any of these fitted forms remains an open question.

B. EOS data for Tl

The present data for the high-pressure phase $cF4$-TlII are illustrated in Fig. 9 in the form of an η-σ plot together with previous data for the same phase from volumetric,[47,48] shock wave,[49] and x-ray measurements at lower pressures.[20,50] In addition also previous volumetric,[47,48] shock wave,[49] and ultrasonic[62,63] data are given for the low-pressure phase $hP2$-TlI. Since the EOS data from shock wave measurements[49] represent only a smooth fitting without taking into account the volume discontinuity at the TlI→TlII phase transition, only the other data are used together with the present results in the least-squares fitting of an $H11$ form to the EOS data for the high-pressure phase $cF4$-TlII. The best fitting values $V_0=0.028(1)$ nm^3, $K_0=29(4)$ GPa, and $K_0'=6.3$ with $\sigma_V=1.3\%$ show just a slight decrease of V_0 with respect to $V_0(hP2\text{-TlI})=0.02852$ nm^3, a small decrease for K_0 with respect to the corresponding (isothermal) value $K_0(hP2\text{-TlI})=35.3$ GPa from ultrasonic measurements, and no significant change in $K_0'(\text{hP2-TlI})=6.2$ when the ultrasonic value for K_0 is used with the form $H11$. Ultrasonic measurements[62] resulted, however, in $K_0'(\text{hP2-TlI})=4.11$, but it is not clear whether the apparent difference between these values for K_0' is really significant with respect to the typical uncertainties of ultrasonic values for K_0'.

V. DISCUSSION

If one compares the present results for structural phase transitions in Ga and Tl under pressure with the theoretical phase diagram for the metallic group-IIIA metals,[19,24,46] one may notice some major discrepancies.

(i) There is no tendency of Tl to enter into a tetragonal phase under pressure.

(ii) The predicted $tI2$-$cF4$ phase transition occurs in Ga only at 85 GPa (at 0 K) in contrast to the much lower predicted transition pressure of about 22 GPa which is obtained with the present EOS data from the predicted critical electron density parameter[46] $r_S=1.98$ a.u. Thereby, $r_S=[3V/(4\pi Z_c)]^{1/3}$ and the conduction electron number $Z_c=3$ are used in the calculation of the corresponding value for V. Also the most recent theoretical study[24] predicts this $tI2$-$cF4$ phase transition at 0 K already at 25 GPa, in contrast to the present data, and the prediction of a $cI12$-$cF4$ phase transition at 14.5 GPa and 0 K with minor temperature effects[24] does not fit to the present experimental data with extended stability of the intermediate $tI2$ phase.

One may thus conclude that the present data for Ga and Tl together with the previous experimental data for In (Refs. 26 and 31) and for Al (Ref. 29) deserve still more detailed structural calculations and also a major revision of the generalized phase diagram[46] for the metallic group-IIIA elements.

If one compares all the available EOS data for the group-IIIA elements in the form of the η-σ representation given in Fig. 10, one can notice that all the data are represented within the present accuracy just by straight lines. These lines interpolate between the low-pressure data and $\eta(0)=0$ for ultimate compression for all the different phases and elements with only minor differences in the slopes for different phases of these elements. Additionally, recent data from neutron diffraction studies on both α- and β-B under pressures up to 10 GPa (Ref. 64) are included in this figure.

On the other hand, a comparison of these EOS data with the (average) behavior of ''ideal'' solids[30] shows also some

systematic trends: First of all, B, with its strong covalent s-p bonds and its semiconducting behavior, is stiffer than all the other group-IIIA elements. This is similar to the special stiffness already observed for the lighter group-IVA elements C, Si, and Ge in their covalent (semiconducting) low-pressure phases.[30,65] In the comparison of Al with Ga, In, and Tl one can notice an extra softness of the heavier elements, where the occupied d bands may contribute some weak additional bonding. This effect is most pronounced for Ga, where the $3d$ band is much lower in comparison with In and Tl, because the $3d$ band is not affected by an additional orthogonality constraint with respect to lower occupied d bands as in the case for the $4d$ and $5d$ bands of In and Tl, respectively. Nevertheless, this additional bonding in the heavier group-IIIA metals appears to be so weak that no special softening under pressure occurs as typically observed for the heavier alkali, earth alkali, and rare earth metals under pressure.[4,9,13] Thus, all the group-IIIA elements with all their high-pressure phases can be described as ''simple'' materials from the point of view of their simple straight line behavior in this η-σ plot. This corresponds to an accurate representation of all their EOS data by the simple EOS form $H11$, which correlates all the higher-order pressure derivatives K_0', K_0'',... just to the starting values V_0 and K_0. Together with the atomic number Z these two values are then only needed for each phase to reproduce all the available EOS data for these elements.

ACKNOWLEDGMENTS

This work has been supported by the Bundesministerium für Wissenschaft und Forschung (BMFT) under Contract No. 05 5P PA XB. The authors would like to thank W. Sievers for technical assistance, J. Otto for support at the EDX station, and the HASYLAB staff for technical help during the stays at HASYLAB-DESY.

[1] A.L. Ruoff, H. Xia, and Q. Xia, Rev. Sci. Instrum. **63**, 4342 (1992).
[2] H. Olijnyk and W.B. Holzapfel, Phys. Lett. **A99**, 381 (1983).
[3] K. Takemura and K. Syassen, Phys. Rev. B **28**, 1193 (1983).
[4] M. Winzenick, V. Vijayakumar, and W.B. Holzapfel, Phys. Rev. B **50**, 12 381 (1994).
[5] H. Olijnyk and W.B. Holzapfel, Phys. Lett. A **100**, 191 (1984).
[6] H. Olijnyk and W.B. Holzapfel, Phys. Rev. B **31**, 4782 (1985).
[7] H. Olijnyk and W.B. Holzapfel, in *High Pressure Geoscience and Material Synthesis*, edited by H. Vollstädt (Academic-Verlag, Berlin, 1988), p. 75.
[8] K. Takemura, Phys. Rev. B **50**, 16 239 (1994).
[9] M. Winzenick and W.B. Holzapfel, in *Proceedings of the Joint XV AIRAPT and XXXIII EHPRG International Conference Warsaw 1995*, edited by W. Trzeciakowski (Polish Academy of Science, Warsaw, 1996), p. 384.
[10] Y.K. Vohra, S.K. Sikka, and W.B. Holzapfel, J. Phys. F **13**, L107 (1983).
[11] H. Xia, G. Parthasarathy, H. Luo, Y.K. Vohra, and A.L. Ruoff, Phys. Rev. B **42**, 6736 (1990).
[12] W.A. Grosshans and W.B. Holzapfel, J. Phys. C **8**, 141 (1984).
[13] T. Krüger, B. Merkau, W.A. Grosshans, and W.B. Holzapfel, High Press. Res. **2**, 193 (1989).
[14] W.A. Grosshans and W.B. Holzapfel, Phys. Rev. B **45**, 5171 (1992).
[15] W.B. Holzapfel, Physica B **190**, 21 (1993).
[16] F. Porsch and W.B. Holzapfel, Phys. Rev. Lett. **70**, 4087 (1993).
[17] Y.C. Zhao, F. Porsch, and W.B. Holzapfel, Phys. Rev. B **49**, 815 (1994).
[18] W.B. Holzapfel, J. Alloys Compounds **223**, 170 (1995).
[19] D.A. Young, *Phase Diagrams of the Elements* (University of California Press, Berkeley, 1991).
[20] O. Schulte, A. Nikolaenko, and W.B. Holzapfel, High Press. Res. **6**, 169 (1991).
[21] J.A. Moriarty, Phys. Rev. B **38**, 3199 (1988).
[22] X.G. Gong, G.L. Chiarotti, M. Parrinello, and E. Tosatti, Phys. Rev. B **43**, 14 277 (1991).
[23] X.G. Gong, G.L. Chiarotti, M. Parrinello, and E. Tosatti, Europhys. Lett. **21**, 469 (1993).
[24] M. Bernasconi and G.L. Chiarotti, Phys. Rev. B **52**, 9988 (1995).
[25] K. Takemura and H. Fujihisa, Phys. Rev. B **47**, 8465 (1993).
[26] S. Meenakshi, B.K. Godwal, R.S. Rao, and V. Vijayakumar, Phys. Rev. B **50**, 6569 (1994).
[27] Structures are labeled according to *Nomenclature of Inorganic Chemistry, International Union of Pure and Applied Chemistry, Recommendations 1990*, edited by G.J. Leigh (Blackwell, Oxford, 1990).
[28] A.K. McMahan and J.A. Moriarty, Phys. Rev. B **27**, 3235 (1983).
[29] R.G. Greene, H. Luo, and A.L. Ruoff, Phys. Rev. B **51**, 597 (1995).
[30] W.B. Holzapfel, Europhys. Lett. **16**, 67 (1991).
[31] O. Schulte and W.B. Holzapfel, Phys. Rev. B **48**, 767 (1993).
[32] O. Schulte and W.B. Holzapfel, Phys. Rev. B **52**, 12 636 (1995).
[33] O. Schulte and W.B. Holzapfel, Phys. Rev. B **53**, 569 (1996).
[34] R.P. Feynman, N. Metropolis, and E. Teller, Phys. Rev. **75**, 1561 (1949).
[35] W.B. Holzapfel and W. May, Adv. Earth Planet. Sci. **12**, 73 (1982).
[36] W.A. Grosshans, E.F. Düsing, and W.B. Holzapfel, High Temp. High Press. **16**, 539 (1984).
[37] J.W. Otto (unpublished).
[38] K. Syassen and W.B. Holzapfel, Europhys. Conf. Abstr. **1A**, 75 (1975).
[39] W.B. Holzapfel, in *High Pressure Chemistry*, edited by H. Kelm (Reidel, Boston, 1978), p. 177.
[40] R.A. Forman, G.J. Piermarini, J.D. Barnett, and S. Block, Science **176**, 284 (1972).
[41] H.K. Mao, P.M. Bell, J.W. Shaner, and J.D. Steinberg, J. Appl. Phys. **49**, 3276 (1978).
[42] J. Donohue, *The Structure of the Elements* (Wiley, New York, 1974).
[43] L. Bosio, A. Defrain, H. Curien, and A. Rimsky, Acta Crystallogr. B **25**, 995 (1969).
[44] L. Bosio, J. Chem. Phys. **68**, 1221 (1978).
[45] F. Porsch (private communication).
[46] J. Hafner and V. Heine, J. Phys. F **13**, 2479 (1983).
[47] P.W. Bridgman, Phys. Rev. **60**, 351 (1941).

[48] S.N. Vaidya and G.C. Kennedy, J. Phys. Chem. Solids **31**, 2329 (1970).
[49] G.C. Kennedy and R.N. Keeler, in *American Institute of Physics Handbook*, 3rd ed. (McGraw Hill, New York, 1972), pp. 4–38.
[50] J.M. Leger and A.M. Redon, High Press. Res. **6**, 233 (1991).
[51] W.B. Holzapfel, Rep. Prog. Phys. **59**, 2151 (1996).
[52] F.D. Murnaghan, *Finite Deformation of an Elastic Solid* (Dover, New York, 1967).
[53] F. Birch, Phys. Rev. **71**, 809 (1947).
[54] P. Vinet, J. Ferrante, J.R. Smith, and J.H. Rose, J. Phys. C **19**, L476 (1986).
[55] W.J. Nellis, J.A. Moriarty, A.C. Mitchell, M. Ross, R.G. Dandrea, N.W. Ashcroft, N.C. Holmes, and R.G. Gathers, Phys. Rev. Lett. **60**, 1414 (1988).
[56] A.C. Mitchell, W.J. Nellis, J.A. Moriarty, R.A. Heinle, N.C. Holmes, and R.E. Tipton, J. Appl. Phys. **69**, 2981 (1991).
[57] A.K. McMahan and M. Ross, in *High Pressure Science and Technology*, edited by K. D. Timmerhaus and M. S. Barber (Plenum, New York, 1979), p. 920.
[58] B.K. Godwal, S.K. Sikka, and R. Chidambaram, Phys. Rev. Lett. **47**, 1144 (1981).
[59] J.C. Boettger and S.B. Trickey, Phys. Rev. B **29**, 6434 (1984).
[60] R. Meyer-Ter-Vehn and W. Zittel, Phys. Rev. B **37**, 8647 (1988).
[61] R.C. Lincoln and A.L. Ruoff, Rev. Sci. Instrum. **44**, 1239 (1973).
[62] M.W. Guinan and D.J. Steinberg, J. Phys. Chem. Solids **35**, 1501 (1974).
[63] R.W. Ferris, M.L. Shepard, and J.F. Smith, J. Appl. Phys. **34**, 768 (1963).
[64] R.J. Nelmes, J.S. Loveday, D.R. Allan, J.M. Besson, G. Hamel, P. Grima, and S. Hull, Phys. Rev. B **47**, 7668 (1993).
[65] G. Queisser and W.B. Holzapfel, Appl. Phys. A **53**, 114 (1991).